Synthesis, Structure, and Magnetism of Mono- and Binuclear Manganese(II) Compounds of Nitronyl Nitroxide Substituted Phosphine Oxides

Corinne Rancurel,[†] Daniel B. Leznoff,[†] Jean-Pascal Sutter,*[,†] Stéphane Golhen,[‡] Lahcène Ouahab,[‡,§] Janis Kliava,[||] and Olivier Kahn*[,†]

Laboratoire des Sciences Moléculaires, Institut de Chimie de la Matière Condensée de Bordeaux, UPR CNRS No. 9048, F-33608 Pessac, France, Groupe Matériaux Moléculaires, UMR CNRS No. 6511, Université Rennes 1, F-35042 Rennes, France, and Centre de Physique Moléculaire Optique et Hertzienne, UMR CNRS Université Bordeaux 1, 351, cours de la Libération, F-33405 Talence, France

Received May 14, 1999

Complexes of manganese(II)-containing aminoxyl radical substituted phosphine oxide ligands are reported. The compounds [(*o*-nitronyl nitroxide-phenyl)diphenylphosphine oxide]bis(hexafluoroacetylacetonato)manganese(II), **3**, and bis{[(*p*-nitronyl nitroxide-phenyl) diphenylphosphine oxide]bis(hexafluoroacetylacetonato)manganese(II)}, **4**, prepared by addition of the free radical phosphine oxides to $Mn(hfac)_2$, were structurally characterized. Complex **3** is mononuclear, containing an O,O-chelating ortho-substituted radical phosphine oxide ligand, while in **4** the para-substituted ligands bridge two $Mn(hfac)_2$ units to yield a binuclear molecular rectangle. The magnetic behavior of both systems is dominated by a strong antiferromagnetic Mn(II)−aminoxyl interaction ($J = -213$ (**3**), -218 (**4**) cm^{-1} with $H = -J\mathbf{S}_{Mn}\cdot\mathbf{S}_{rad}$) to give effective $S = 2$ ground state units. The $S = 3$ excited state is populated at high temperatures. At low temperatures a decrease in $\chi_M T$ in both complexes is attributable primarily to inter- or intramolecular antiferromagnetic interactions rather than zero-field splitting (ZFS) of the $S = 2$ ground state. For the bimetallic compound, the magnetic data indicate that ligand-mediated interactions between the Mn(II) spin carriers are weak. The powder EPR spectra of both systems have been recorded and successfully simulated, giving a ZFS parameter $D = 0.112$ cm^{-1}. Crystals of **3** are triclinic, space group $P\bar{1}$ with $a = 10.6672(19)$ Å, $b = 13.270(6)$ Å, $c = 15.363(3)$ Å, $\alpha = 93.84(2)°$, $\beta = 108.054(16)°$, $\gamma = 105.69(3)°$, and $Z = 2$. Crystals of **4** are monoclinic, space group $P2_1/a$ with $a = 12.463(6)$ Å, $b = 19.315(3)$ Å, $c = 17.084(9)$ Å, $\alpha = 90°$, $\beta = 98.49(2)°$, $\gamma = 90°$, and $Z = 2$.

Introduction

Nitronyl nitroxides, stable organic radicals,[1,2] have played a prominent role in the design and construction of molecular magnetic materials.[3] The "metal−organic" strategy of combining organic radicals with paramagnetic transition metal ions has been particularly successful, and a wide variety of species utilizing nitronyl nitroxides as ligands have been described.[4,5] The recognized weak basicity of the nitroxide functionality has led to the development of numerous nitroxides in which a strong coligand is incorporated.[6] Most such coligands are nitrogen-based donors, in particular planar N-heterocycles (e.g., pyridine,[7] imidazole,[8] triazole[9]). Using a wide range of such ligands, it has been shown that the ligand regiochemistry plays an important role in the determination of the structure and magnetic properties of subsequent metal complexes. Hence $Mn(hfac)_2$ complexes (hfac = hexafluoroacetylacetonate) with various nitronyl nitroxide ligands exhibit a variety of structures, including mononuclear chelating systems,[10−12] chains,[13−16] planes,[8] and supramolecular rings;[17] bridging *t*-BuNO ligands have been utilized in a similar fashion.[18,19] Pyridine-substituted

* To whom correspondence should be addressed.
[†] Institut de Chimie de la Matière Condensée de Bordeaux.
[‡] Université Rennes 1.
[§] Author for inquiries relating to the crystallographic studies.
[||] Université Bordeaux 1.

(1) Osiecki, J. H.; Ullman, E. F. *J. Am. Chem. Soc.* **1968**, *90*, 1078.
(2) Ullman, E. F.; Osiecki, J. H.; Boocock, D. G. B.; Darcy, R. *J. Am. Chem. Soc.* **1972**, *94*, 7049.
(3) Kahn, O. *Molecular Magnetism*; VCH: Weinheim, 1993.
(4) Caneschi, A.; Gatteschi, D.; Sessoli, R.; Rey, P. *Acc. Chem. Res.* **1989**, *22*, 392.
(5) Caneschi, A.; Gatteschi, D.; Rey, P. *Prog. Inorg. Chem.* **1991**, *39*, 331.
(6) Larionov, S. V. *J. Struct. Chem.* **1983**, 594.
(7) Lanfranc de Panthou, F.; Belorizky, E.; Calemezuk, R.; Luneau, D.; Marcenat, C.; Ressouche, E.; Turek, P.; Rey, P. *J. Am. Chem. Soc.* **1996**, *117*, 11247.
(8) Fegy, K.; Luneau, D.; Ohm, T.; Paulsen, C.; Rey, P. *Angew. Chem., Int. Ed.* **1998**, *37*, 1270.
(9) Sutter, J.-P.; Kahn, M. L.; Golhen, S.; Ouahab, L.; Kahn, O. *Chem.−Eur. J.* **1998**, *4*, 571.
(10) Caneschi, A.; Gatteschi, D.; Renard, J. P.; Rey, P.; Sessoli, R. *Inorg. Chem.* **1989**, *28*, 3314.
(11) Fegy, K.; Sanz, N.; Luneau, D.; Belorizky, E.; Rey, P. *Inorg. Chem.* **1998**, *37*, 4518.
(12) Luneau, D.; Risoan, G.; Rey, P.; Grand, A.; Caneschi, A.; Gatteschi, D.; Laugier, J. *Inorg. Chem.* **1993**, *32*, 5616.
(13) Schiødt, N. C.; de Biani, F. F.; Caneschi, A.; Gatteschi, D. *Inorg. Chim. Acta* **1996**, *248*, 139.
(14) Lee, C.-J.; Huang, C.-H.; Wei, H.-H.; Liu, Y.-H.; Lee, G.-H.; Wang, Y. *J. Chem. Soc., Dalton Trans.* **1998**, 171.
(15) Caneschi, A.; Ferraro, F.; Gatteschi, D.; Rey, P.; Sessoli, R. *Inorg. Chem.* **1991**, *30*, 3162.
(16) Caneschi, A.; Gatteschi, D.; Rey, P.; Sessoli, R. *Inorg. Chem.* **1991**, *30*, 3936.
(17) Caneschi, A.; Gatteschi, D.; Laugier, J.; Rey, P.; Sessoli, R.; Zanchini, C. *J. Am. Chem. Soc.* **1988**, *110*, 2795.
(18) Iwamura, H.; Inoue, K.; Koga, N. *New J. Chem.* **1998**, *22*, 201.
(19) Inoue, K.; Hayamizu, T.; Iwamura, H.; Hashizume, D.; Ohashi, Y. *J. Am. Chem. Soc.* **1996**, *118*, 1803.

10.1021/ic990527g CCC: $18.00
Published on Web 09/29/1999

nitronyl nitroxides and *t*-Bu-aminoxyls[20,21] have been particularly instructive in examining structural and magnetic changes that occur with different regiochemical substitution patterns.

In light of the intense focus on metal−radical systems, it is interesting to note that phosphorus-based donors have been conspicuously absent in nitronyl nitroxide chemistry. Phosphorus ligands offer several differences compared with more traditional nitrogen heterocycle donors, including their pseudotetrahedral geometry and their wide-ranging coordination chemistry.[22] In response, we have recently described the synthesis of novel phosphine[23,24] and phosphine oxide[25] substituted nitronyl nitroxides. The phosphine derivatives were shown to coordinate selectively via the P atom to soft, low-valent metal centers without alteration of the radical moiety.[23,26] Here we focus on the triphenylphosphine oxide ligands. As a useful comparison to the pyridine systems, the coordination chemistry of both *o*- and *p*-nitronyl nitroxide substituted triphenylphosphine oxides with $Mn(hfac)_2$ is hereby presented and reveals differences in both structure and magnetic properties. The results indicate the importance of ligand topology in controlling the complex structure.

Experimental Section

General Procedures. Unless otherwise stated all manipulations were performed in air using purified solvents. CH_2Cl_2 was heated to reflux over CaH_2 under a nitrogen atmosphere and distilled prior to use. Heptane was prewashed with H_2SO_4 and $KMnO_4$ and distilled from sodium. The nitronyl nitroxide substituted triphenylphosphine oxide ligands **1** and **2** were prepared as previously described.[25] $Mn(hfac)_2 \cdot 3H_2O$ was obtained from TCI Chemicals. Infrared spectra were collected on a Perkin-Elmer FT-IR Pergamon 1000 spectrometer. EPR spectra were collected on a Bruker EMX spectrometer operating in the X-band (9.3 GHz) equipped with an Oxford ESR-900 flowing-helium cryostat (4.2−300 K) controlled by an Oxford ITC4 temperature control unit. EPR spectra were simulated using a program described in the text. The line shape has been approximated with a Gaussian derivative curve with a 200 Oe peak-to-peak width. Elemental analyses were conducted by the central CNRS microanalysis service (Lyon). Magnetic susceptibility data were measured using a SQUID MPMS-5S magnetometer working down to 2 K at 1000 Oe field strength. The data were corrected for the diamagnetism of the constituent atoms.

Synthesis of [(*o*-Nitronyl nitroxide-phenyl)diphenylphosphine oxide]bis(hexafluoroacetylacetonato)manganese(II), $Mn(hfac)_2$-[*o*PONit] (3). $Mn(hfac)_2 \cdot 3H_2O$ (0.120 g, 0.230 mmol) was suspended in heptane (30 mL) and heated at 95 °C for 45 min, with concurrent evaporation of the H_2O/heptane azeotrope, to give a yellow solution of $Mn(hfac)_2$. This solution was allowed to cool under nitrogen to room temperature, and then a 5 mL CH_2Cl_2 solution of phosphine oxide **1** (0.100 g, 0.230 mmol) was added, with stirring, to yield a purple precipitate. The reaction mixture was filtered in air to yield a purple filtrate. Slow evaporation of this heptane/CH_2Cl_2 solution gave red crystals of **3** suitable for X-ray analysis. Yield: 0.062 g (30%). Anal. Calcd for $C_{35}H_{28}N_2F_{12}MnO_7P$: C, 46.58; H, 3.12; N, 3.10. Found: C, 47.02; H, 3.39; N, 2.95. IR (KBr): 1648, (s, C═O), 1525 (m), 1507 (m), 1356 (m, N−O), 1256 (s, C−F), 1194 (s, P═O), 1145 (s), 796 (w), 664 (w), 548 (w) cm^{-1}.

Table 1. Summary of Crystallographic Data

	3	**4**
formula	$C_{35}H_{28}F_{12}MnN_2O_7P$	$C_{70}H_{56}F_{24}Mn_2N_4O_{14}P_2$
fw	902.50	1805.101
temp, K	293	293
space group	$P\bar{1}$	$P2_1/a$
a, Å	10.6672(19)	12.463(6)
b, Å	13.270(6)	19.315(3)
c, Å	15.363(3)	17.084(9)
α, deg	93.84(2)	90
β, deg	108.054(16)	98.49(2)
γ, deg	105.69(3)	90
V, Å^3	1963.2(10)	4067(3)
Z	2	2
ρ_{calc}, g/cm^3	1.527	1.474
μ, mm^{-1}	0.482	0.466
λ, Å	0.710 73	0.710 73
R1, wR2 ($I \geq 2\sigma(I)$)[a]	0.0697, 0.1920	0.0675, 0.1728
R1, wR2 (all data)[a]	0.1634, 0.2342	0.1699, 0.2174

[a] Function minimized: $\sum w(|F_o^2 - F_c^2|)^2$ where $w^{-1} = \sigma^2(F_o^2)$, $R = \sum||F_o| - |F_c||/\sum|F_o|$, $wR2 = (\sum w(F_o^2 - F_c^2)^2/\sum w(F_o^2)^2)^{1/2}$.

Synthesis of Bis{[(*p*-nitronyl nitroxide-phenyl)diphenylphosphine oxide]bis(hexafluoroacetylacetonato)manganese(II)}, {$Mn(hfac)_2$-[*p*PONit]}$_2$ (4). $Mn(hfac)_2 \cdot 3H_2O$ (0.047 g, 0.090 mmol) was suspended in heptane (15 mL) and heated at 95 °C, with concurrent evaporation of the H_2O/heptane azeotrope, for 30 min to give a yellow solution of $Mn(hfac)_2$. This solution was allowed to cool under nitrogen to 40 °C, and then a 2 mL CH_2Cl_2 solution of phosphine oxide **2** (0.043 g, 0.099 mmol) was added, with stirring, to yield a green precipitate. The reaction mixture was filtered in air, and the precipitate was redissolved in a minimum amount of CH_2Cl_2 and was added to the filtrate. Slow evaporation of this heptane/CH_2Cl_2 solution gave green crystals of **4** suitable for X-ray analysis. Yield: 0.080 g (90%). Anal. Calcd for $C_{70}H_{56}N_4F_{24}Mn_2O_{14}P_2$: C, 46.58; H, 3.12; N, 3.10. Found: C, 46.70; H, 3.31; N, 3.08. IR (KBr): 1657 (m, C═O), 1653 (m, C═O), 1506 (m), 1360 (w, N−O), 1355 (w, N−O), 1256 (s, C−F), 1196 (s, P═O), 1146 (s), 794 (w), 663 (w), 550 (w) cm^{-1}.

X-ray Crystallographic Analysis. Single crystals of red **3** and green **4** were mounted at the end of glass fibers. Cell dimensions and orientation matrices for data collection were obtained from least-squares refinement, using the setting angles of 25 centered reflections. For both compounds, intensity data were collected at room temperature on an Enraf-Nonius CAD-4 diffractometer equipped with a Mo Kα source (λ = 0.710 73 Å) and graphite monochromator, employing the $\theta-2\theta$ technique. After a semiempirical φ-scan[27] absorption correction, the data reduction was performed using MolEN[28] while structure solutions and refinements were carried out using the SHELXS-86 and SHELXL-97 programs.[29] For compound **3**, the two hfac units were restrained to be similar. Hydrogen atoms were located on the basis of geometrical considerations and treated according to the riding model during refinement, with isotropic displacement corresponding to the heavy atom to which they were linked. For compound **3**, hydrogen atoms were refined isotropically. Crystallographic and refinement parameters are given in Table 1. Selected bond lengths and angles are given in Table 2.

Results and Discussion

Synthesis and Structure of $Mn(hfac)_2$ Complexes with Nitronyl Nitroxide Phosphine Oxides. The synthesis of $Mn(hfac)_2$ adducts with nitronyl nitroxide substituted phosphine oxide ligands **1** (*o*PONit) and **2** (*p*PONit) is accomplished in a

(20) Ishimaru, Y.; Kitano, M.; Kumada, H.; Koga, N.; Iwamura, H. *Inorg. Chem.* **1998**, *37*, 2273.
(21) Kitano, M.; Ishimaru, Y.; Inoue, K.; Koga, N.; Iwamura, H. *Inorg. Chem.* **1994**, *33*, 6012.
(22) Cotton, F. A.; Wilkinson, G. *Advanced Inorganic Chemistry*, 5th ed.; John Wiley & Sons: New York, 1988.
(23) Rancurel, C.; Sutter, J.-P.; Le Hoerff, T.; Ouahab, L.; Kahn, O. *New J. Chem.* **1998**, *22*, 1333.
(24) Leznoff, D. B.; Rancurel, C.; Sutter, J.-P.; Golhen, S.; Ouahab, L.; Rettig, S. J.; Kahn, O. *Mol. Cryst. Liq. Cryst.* **1999**, *334*, 425.
(25) Rancurel, C.; Sutter, J.-P.; Kahn, O.; Guionneau, P.; Bravic, G.; Chasseau, D. *New J. Chem.* **1997**, *21*, 275.
(26) Leznoff, D. B.; Rancurel, C.; Sutter, J.-P.; Rettig, S. J.; Pink, M.; Paulsen, C.; Kahn, O. *J. Chem. Soc., Dalton Trans.*, in press.
(27) North, A. C. T.; Philips, D. C.; Mathews, F. S. *Acta Crystallogr., Sect. A* **1968**, *A24*, 351.
(28) *MolEN (Molecular Structure Enraf-Nonius)*; Enraf-Nonius: Delft, The Netherlands, 1990.
(29) (a) Sheldrick, G. M. *SHELXS-86: Program for the Solution of Crystal Structures*; University of Göttingen: Göttingen, Germany, 1986. (b) Sheldrick, G. M. *SHELXL-97: Program for the Refinement of Crystal Structures*; University of Göttingen: Göttingen, Germany, 1997.

Table 2. Selected Bond Lengths (Å) and Angles (deg) for $Mn(hfac)_2$(*o*PONit) (**3**) and $[Mn(hfac)_2$(*p*PONit)$]_2$ (**4**)[a]

	3	**4**
Mn(1)−O(2)	2.150(4)	2.142(3)
Mn(1)−O(3)	2.222(4)	2.153(4)
Mn(1)−O(4)	2.144(4)	2.181(4)
Mn(1)−O(5)	2.147(3)	2.177(4)
Mn(1)−O(6)	2.159(3)	2.140(4)
Mn(1)−O(7)	2.089(3)	2.076(4)
P(1)−O(7)	1.492(3)	1.486(4)
N(1)−O(1)	1.261(5)	1.283(6)
N(2)−O(2)	1.297(4)	1.294(5)
N(1)−C(7)	1.348(6)	1.342(6)
N(2)−C(7)	1.333(5)	1.340(6)
C(1)−C(7)	1.474(6)	1.471(7)
O(2)−Mn(1)−O(3)	178.14(13)	90.58(15)
O(2)−Mn(1)−O(4)	97.46(15)	98.62(14)
O(2)−Mn(1)−O(5)	88.93(14)	175.28(16)
O(2)−Mn(1)−O(6)	97.29(14)	93.86(14)
O(2)−Mn(1)−O(7)	88.44(13)	83.13(15)
O(3)−Mn(1)−O(4)	80.85(15)	81.60(15)
O(3)−Mn(1)−O(5)	92.12(15)	87.82(18)
O(3)−Mn(1)−O(6)	84.37(15)	95.36(15)
O(3)−Mn(1)−O(7)	90.70(14)	167.88(16)
O(4)−Mn(1)−O(5)	99.54(14)	85.54(16)
O(4)−Mn(1)−O(6)	165.13(16)	167.17(15)
O(4)−Mn(1)−O(7)	87.53(14)	89.09(15)
O(5)−Mn(1)−O(6)	82.56(13)	81.88(16)
O(5)−Mn(1)−O(7)	172.72(14)	99.23(18)
O(6)−Mn(1)−O(7)	91.04(13)	95.39(15)
N(2)−O(2)−Mn(1)	124.7(3)	126.6(3)
P(1)−O(7)−Mn(1)	146.2(2)	152.7(3)
O(1)−N(1)−C(7)	125.7(4)	126.3(5)
O(2)−N(2)−C(7)	125.7(4)	125.5(4)
N(1)−C(7)−N(2)	108.9(4)	127.2(4)

[a] Symmetry transformations used to generate equivalent atoms in **4**: $-x+2, -y+1, -z+1$.

straightforward manner via addition of the ligands to anhydrous $Mn(hfac)_2$ followed by slow crystallization from a heptane/CH_2Cl_2 solution (eqs 1 and 2). The crystals thereby obtained were suitable for X-ray analysis, and the structures of the two complexes **3** and **4** were solved.

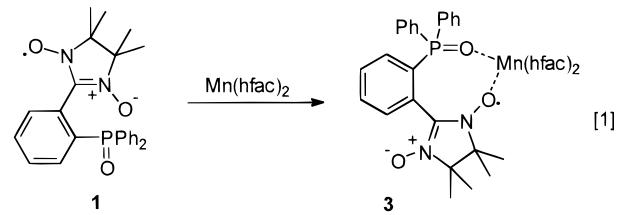

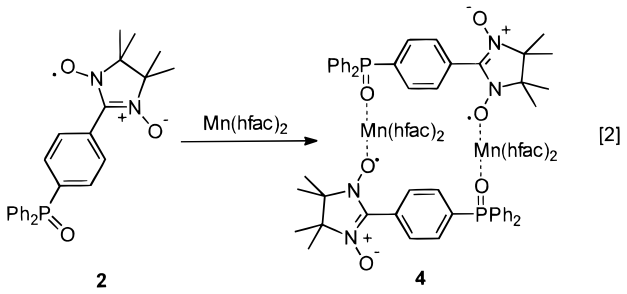

The presence in aminoxyl derivatives of a functional group able to act as a coligand has been shown to enhance the coordination behavior of the radical moiety to a metal center. This is especially true if the ligand can form a chelate to the metal. In phospine oxide **1** the nitronyl nitroxide moiety and the intramolecular coligand phosphine oxide unit are ortho to each other, a favorable situation to have the molecule functioning as an *O,O*-chelating ligand. Indeed, phosphine oxide **1** forms mononuclear complex **3** with $Mn(hfac)_2$ in which the manganese(II) center is octahedrally coordinated by six oxygen atoms (Figure 1). The phosphine oxide and aminoxyl moieties are cis-coordinated (the O(2)−Mn(1)−O(7) angle is 88.44(13)°). The four Mn−O(hfac) bond lengths range from 2.144(4) to 2.222(4) Å (Table 2). The Mn−O(7) (phosphine oxide) bond length of 2.089(3) Å is slightly longer than the 2.069(6) Å found in $MnCl_2(OPPh_3)_2$.[30] The Mn−O(2) (aminoxyl) bond length of 2.150(4) Å is typical of those found in similar systems. The two N−O groups have bond lengths of 1.297(4) and 1.261(5) Å for coordinated and uncoordinated nitroxides, respectively, as is generally observed.[5] The twist angle between the nitronyl nitroxide plane and the phenyl group to which it is bound is 62.8° in the free ligand **1**,[25] indicating that the steric hindrance of the two donor groups forces the ligand into a nearly orthogonal conformation. This twist is exacerbated upon metal complexation to 75°. This is in stark contrast to the *o*-nitronyl nitroxide substituted pyridine ligand, where twist angles of 28−35° are observed in both the free ligand and its metal complexes.[12,31] Despite the ligand distortion, the Mn−O(2)−N(2) angle of 124.7(3)° indicates that a significant overlap between the π orbitals of the N−O group and the Mn d orbitals will still be operative. The chelate effect observed with phosphine oxide **1** allows one to envisage the use of a related phosphine derivative in order to induce the coordination of an aminoxyl radical to a soft metal center.

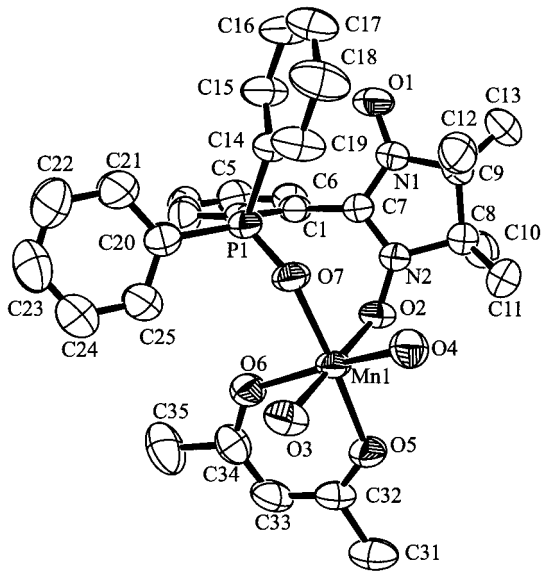

Figure 1. Molecular structure (ORTEP, 33% ellipsoids) and numbering scheme for $Mn(hfac)_2$[*o*PONit] (**3**). Except for its O atoms, one hfac ligand has been removed for clarity.

Altering the ligand regiochemistry from ortho to para substitution (ligand **2**) and subsequent reaction with $Mn(hfac)_2$ gives compound **4**. The structure of this bimetallic species (Figure 2) reveals the formation of a molecular rectangle, or cyclic dimer, with the phosphine oxide ligand forming the long edge of the rectangle, and the Mn(II) centers in the middle of the short sides. Each ligand is bridging two Mn centers, by virtue of N−O bonding to one Mn and P═O bonding to the other. The two phenyl rings forming the long edges are π-stacked,

(30) Tomita, K. *Acta Crystallogr. C* **1985**, *C41*, 1832.
(31) Caneschi, A.; Ferraro, F.; Gatteschi, D.; Rey, P.; Sessoli, R. *Inorg. Chem.* **1990**, *29*, 1756.

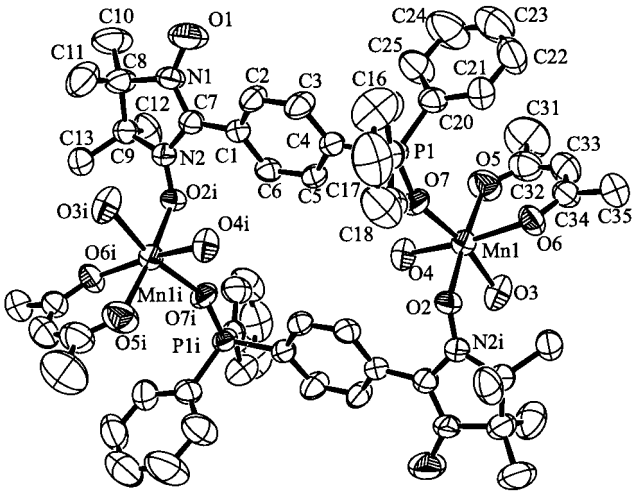

Figure 2. Molecular structure (ORTEP, 33% ellipsoids) and numbering scheme for $[Mn(hfac)_2(p\text{PONit})]_2$ (**4**). Except for its O atoms, one hfac ligand per Mn center has been removed for clarity.

with a distance of 6.25 Å between the planes. The distance between Mn(II) centers is 8.46 Å; each Mn(II) is again octahedrally coordinated with oxygen atoms, with the phosphine oxide and nitronyl nitroxide oxygens in a cis orientation (the O(2)−Mn−O(7) angle is 83.13(15)°). The Mn−O(7) (phosphine oxide) and P(1)−O(7) bond lengths of 2.076(4) and 1.486(4) Å compare well with the 2.069(6) and 1.488(8) Å bond lengths found in $MnCl_2(OPPh_3)_2$ [30] and with the P−O bond length of 1.482(2) Å in the free ligand.[25] The Mn−O(2) (nitroxide) bond length of 2.142(3) Å is typical of those found in similar systems and compares well with the 2.150(4) Å found in **3**. The two N−O groups have bond lengths of 1.294(5) and 1.283(6) for coordinated and uncoordinated nitroxides, respectively, a smaller difference than that observed in **3**. The 27° twist angle in **4** between the nitronyl nitroxide plane and the phenyl group to which it is bound is 28.3° in the free ligand **2**; there is hence little strain in the ligand framework upon ligation. The Mn−O(2)−N(2) angle of 126.6(3)° indicates that good overlap between the magnetic orbitals exists. There are no significant intermolecular contacts in either structure. The shortest distance between N−O groups in **4** is 5.13 Å; in **3** it is 5.97 Å.

The formation of a molecular rectangle in this system is facilitated by the topology of phosphine oxide **2**, which could be described as "C-shaped"; the ligand backbone forms the long side of the C while the P═O and N−O donor moieties complete the C. The similar *p*-nitronyl nitroxide substituted pyridine ligand has "L-shaped" topology by virtue of the N−O and pyridine N donor being at roughly right angles to each other.[31] Despite this, reaction of the pyridine ligand with $Mn(hfac)_2$ in a 1:1 ratio also yields a molecular rectangle. In this case, however, the Mn nuclei are located at two opposite corners of the rectangle as opposed to within the sides; the overall rectangle is also smaller in size.[32] These differences are dictated by the ligand topology and also by the metal and its ancillary ligands. For example, reaction of the same pyridine ligand with $HgBr_2$ yields not a molecular rectangle but a mononuclear, three-coordinate complex.[14] A related ligand, 4-*t*-BuNO-pyridine, also forms molecular rectangles when reacted (1:1) with $Mn(hfac)_2$. As above, the "L-topology" of the ligand favors a smaller rectangle than is observed in **4**.[21] The reaction of 4-*t*-BuNO-pyridine with $Cu(hfac)_2$ yields a similar cyclic dimer in which

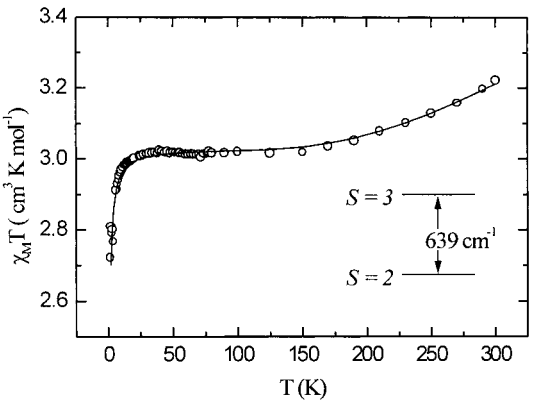

Figure 3. Temperature dependence of $\chi_M T$ for **3**. The solid line corresponds to the best fit of the magnetic data. The inset shows the energy splitting between the $S = 2$ ground and $S = 3$ excited states, as observed at high temperature.

the two monomers are more weakly associated.[20] A molecular rectangle using a bridging bis-aminoxyl radical and $Mn(hfac)_2$ has also been reported.[33] These cyclic complexes are important from a magnetic point of view as they serve as discrete model systems for more intricate polymeric systems (see magnetism below). Diamagnetic molecular squares and rectangles have been widely reported,[34,35] using platinum and palladium complexes and recently, rhenium centers.[36,37]

Magnetic Behavior. $Mn(hfac)_2[o\text{PONit}]$ (3). The temperature (T) dependence of the molar magnetic susceptibility (χ_M) of **3** is shown in Figure 3 as a plot of $\chi_M T$ vs T. At 300 K, $\chi_M T$ is equal to 3.25 cm^3 K mol^{-1}, a value much lower than that expected for non-interacting $S_{Mn} = {}^5/_2$ and $S_{rad} = {}^1/_2$ spins. As the temperature is lowered to 150 K, $\chi_M T$ gradually decreases to reach a plateau value of 3.0 cm^3 K mol^{-1}. This remains stable until approximately 20 K, at which point $\chi_M T$ decreases again slightly to reach 2.7 cm^3 K mol^{-1} at 2 K.

The profile of this curve indicates that, as expected,[5] the Mn(II)−nitroxide radical interaction is strongly antiferromagnetic, leading to a $S = 2$ ground state and a $S = 3$ excited state for the molecule. At room temperature, the $S = 3$ state is weakly populated. The decrease in $\chi_M T$ below 20 K could be attributed to both weak intermolecular antiferromagnetic interactions and zero-field splitting (ZFS) of the $S = 2$ ground state. Such ZFS is indeed observed by EPR (see below).

The magnetic behavior of **3** has been analyzed with a theoretical expression taking into account an intramolecular magnetic interaction between Mn(II) and the radical ligand. At high temperature, the spin Hamiltonian appropriate to this system is given in eq 3, where all symbols have their usual meaning.[3]

$$H = -J\mathbf{S}_{Mn}\cdot\mathbf{S}_{rad} + (g_{Mn}\mathbf{S}_{Mn} + g_{rad}\mathbf{S}_{rad})\beta\mathrm{H} \qquad (3)$$

Taking g_{Mn} and g_{rad} equal to 2.0, the expression of the molar susceptibility is given in eq 4, in which the intermolecular interactions have been considered in the mean-field approximation as zJ'. Least-squares fitting of the experimental data leads

(32) Caneschi, A.; Gatteschi, D.; Sessoli, R.; Rey, P. *Inorg. Chim. Acta* **1991**, *184*, 67.
(33) Görlitz, G.; Hayamizu, T.; Itoh, T.; Matsuda, K.; Iwamura, H. *Inorg. Chem.* **1998**, *37*, 2083.
(34) Fujita, M.; Nagao, S.; Iida, M.; Ogata, K.; Ogura, K. *J. Am. Chem. Soc.* **1993**, *115*, 1574.
(35) Stang, P. J.; Olenyuk, B. *Acc. Chem. Res.* **1997**, *30*, 502.
(36) Benkstein, K. D.; Hupp, J. T.; Stern, C. L. *Inorg. Chem.* **1998**, *37*, 5404.
(37) Woessner, S. M.; Helms, J. B.; Shen, Y.; Sullivan, B. P. *Inorg. Chem.* **1998**, *37*, 5406.

$$\chi_M = \frac{N_g{}^2\beta^2 F}{kT - zJ'F} \quad \text{where} \quad F = \frac{28 + 10e^{-3J/kT}}{7 + 5e^{-3J/kT}} \qquad (4)$$

to $J = -213$ cm^{-1} and $zJ' = -0.09$ cm^{-1}. The energy gap between the $S = 3$ and $S = 2$ states is then equal to 639 cm^{-1}. The value of $J = -213$ cm^{-1} is consistent with those measured in other [nitronyl nitroxide−Mn(hfac)$_2$] systems but, interestingly, is much larger than that found for the related [*o*-(nitronyl nitroxide)-pyridine]Mn(hfac)$_2$. In this latter compound, the abnormally low J value of -65 cm^{-1} was attributed to the angle between the Mn−O−N plane and the nitronyl nitroxide fragment being only 45°, thus reducing the overlap between magnetic orbitals.[12] In **3** this angle is 94.5°, more in line with regularly observed values.

An attempt was made to consider the low-temperature behavior supposing only the zero-field splitting of the $S = 2$ ground state. The low-temperature data could indeed be modeled using the spin Hamiltonian given in eq 5. Neglecting E with

$$H = g\beta H\mathbf{S} + D[S_z{}^2 - (1/3)S(S+1)] + E(S_x{}^2 - S_y{}^2) \qquad (5)$$

respect to D results in the expression of the molar susceptibility in eq 6, where $x = D/kT$.[38] However, this modeling procedure

$$\chi_M = \frac{1}{3}\left[\frac{Ng^2\beta^2(2e^{-x} + 8e^{-4x})}{kT(1 + 2e^{-x} + 2e^{-4x})}\right] + \frac{2}{3}\left[\frac{Ng^2\beta^2[(6/x)(1 - e^{-x}) + (4/3x)(e^{-x} - e^{-4x})]}{kT(1 + 2e^{-x} + 2e^{-4x})}\right] \qquad (6)$$

led to a ZFS parameter $D = 1.38$ cm^{-1}, a value more than 1 order of magnitude larger than the ZFS parameter deduced from the EPR measurements (see below). Hence it is clear that the decrease in $\chi_M T$ at low T cannot be entirely due to ZFS and must thus be attributed mostly to weak intermolecular antiferromagnetic interactions.

{Mn(hfac)$_2$[*p*PONit]}$_2$ (4). The temperature dependence of the magnetic susceptibility of **4** is shown in Figure 4. The $\chi_M T$ vs T plot for dimeric **4** is qualitatively similar to that for monomeric **3**. At 300 K, $\chi_M T$ is equal to 6.4 cm^3 K mol^{-1} and gradually decreases to a plateau value of 6.04 cm^3 K mol^{-1} at 150 K, consistent with two noninteracting $S = 2$ spin states. These are generated by the strong antiferromagnetic coupling within each Mn(II)/radical pair. Modeling the high-temperature data using the same equation as for **3** (eq 4) yields $J = -218$ cm^{-1}; this is similar to that found in **3**. Again, $\chi_M T$ decreases below 20 K to a final value of 5.85 cm^3 mol^{-1} K at 2 K. By employing the same procedure as for **3**, we determined that the decrease in $\chi_M T$ at low temperature in **4** is due primarily to antiferromagnetic interactions and not ZFS of the $S = 2$ states. The magnitude of this interaction was found to be $zJ' = -0.03$ cm^{-1} for **4**. Whether this interaction is intramolecular, mediated by the ligand via the P═O bond, or intermolecular cannot be unambiguously determined from the data. However, it is fairly clear that the intramolecular interaction, if any, between the $S = 2$ pairs is quite weak. With *p*-(nitronyl nitroxide)-pyridine,[15,31,32,39] coupling through the ligand was found to be nonnegligible. Conversely, a *p*-(nitronyl nitroxide) substituted benzaldehyde complex with Mn(hfac)$_2$ showed no significant coupling through the ligand.[40] In complexes with the ligand *p*-(*t*-BuNO)-pyridine,[21] through-ligand interactions were found to be stronger. In a *p*-(*t*-BuNO)-pyridine Cu(hfac)$_2$ species the direct and ligand-mediated coupling were nearly of equal strength.[20]

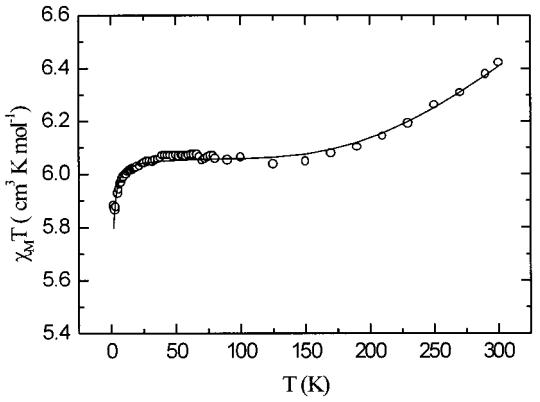

Figure 4. Temperature dependence of $\chi_M T$ for **4**. The solid line corresponds to the best fit of the magnetic data.

The magnetics of the molecular rectangle **4**, indicating little interaction between pairs, is also instructive as a model for extended systems, or compounds with multiple paramagnetic ligands.[11,41] The deconvolution of multiple interactions in such species is challenging, and hence the examination of discrete model systems like **3** and **4** provides valuable information. In this specific case, for example, through-ligand coupling could be nominally discarded as an important parameter. This would likely be equally applicable for extended systems utilizing **1** or **2**.

EPR Spectra. EPR spectra of **3** and **4** in CH_2Cl_2 solution show only dissociated ligand (standard five-line nitronyl nitroxide pattern) and a broad Mn(II) signal. However, EPR powder spectra, recorded at the X-band at 4, 100, and 300 K, show features between 0 and 6000 Oe associated with the compounds. Between 4 and 100 K there is no temperature dependence of the spectral shape. According to the magnetic susceptibility data, the EPR spectrum at 100 K corresponds to a $S = 2$ state. At 300 K the spectrum presents some additional features in the $g = 2$ region (3375 Oe) which may be attributed to the presence of transitions within a thermally accessible $S = 3$ state.

The main absorption features of **3** and **4** are clearly located in the same region (Figure 5). The similarity of the spectra has to be related to the similarity of the paramagnetic units responsible for the EPR absorption in the two compounds, namely, the Mn(II)−nitroxide radical moiety. No resolved hyperfine structure is observed in the spectra, so that the paramagnetic center can be described by the spin Hamiltonian in eq 5.

Extracting the spin Hamiltonian parameters from powder EPR spectra with ZFS is a challenging endeavor. We have computer simulated the experimental spectra using a laboratory-developed computer program for paramagnetic centers described by the spin Hamiltonian H of eq 5 with $S = 2$. The complex H matrix is solved by the well-known Jacobi method. The simulation program carries out a repeated search for resonance magnetic fields $H_r(D,E,\vartheta,\varphi)$ yielding the energy-level separations that match the microwave quantum value, ϑ and φ being the polar and azimuthal angles of the static magnetic field H with respect to the principal axes of a center. The random orientation of

(38) O'Connor, C. J. *Prog. Inorg. Chem.* **1982**, 203.
(39) Chen, Z. N.; Qiu, J.; Gu, J. M.; Wu, M. F.; Tang, W. X. *Inorg. Chim. Acta* **1995**, *233*, 131.
(40) Caneschi, A.; Gatteschi, D.; Sessoli, R. *Inorg. Chem.* **1993**, *32*, 4612.
(41) Fegy, K.; Luneau, D.; Belorizky, E.; Novak, M.; Tholence, J.-L.; Paulsen, C.; Ohm, T.; Rey, P. *Inorg. Chem.* **1998**, *37*, 4524.

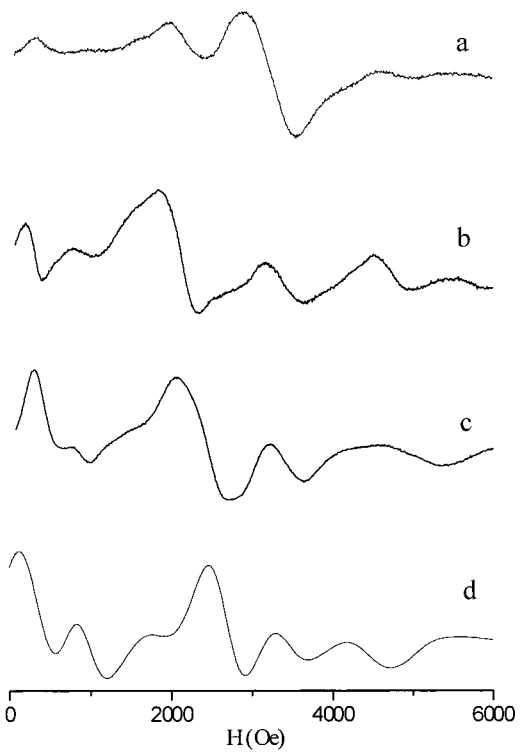

Figure 5. Observed powder EPR spectra for (a) **3** at 300 K, (b) **3** at 100 K, and (c) **4** at 100 K. (d) Simulated powder EPR spectrum of the $S = 2$ state.

paramagnetic centers with respect to the static magnetic field is accounted for by a regular grid of sin ϑ and φ values used in diagonalizing the H matrix. The derivative-of-absorption powder spectra are generated in accordance with eq 7 where $W(D,E,\vartheta,\varphi)$ is the transition intensity calculated using the eigenvectors of H and averaged over all directions of the microwave magnetic field and $F[H - H_r(D,E,\vartheta,\varphi),\Delta H]$ is the line shape which has been chosen as a Gaussian derivative with a peak-to-peak width ΔH.

$$P(H,D,E) = \int_0^{2\pi}\int_0^{\pi} W(D,E,\vartheta,\varphi)F[H - H_r(D,E,\vartheta,\varphi),\Delta H] \sin\vartheta \, d\vartheta \, d\varphi \quad (7)$$

Assuming an isotropic g value of 2.0 for the $S = 2$ ground state, the ZFS parameters for **3** have been estimated by successive comparisons between experimental and simulated spectra to give $D = 0.112$ cm^{-1} and $E = 0.02$ cm^{-1}. We did not attempt to vary the value of g since in a powder spectrum the anisotropy of g should have roughly the same effects as small variations in the D and E parameters. Experimental and simulated spectra are compared in Figure 5. The agreement between the two spectra, although not perfect, is fairly good. It is evident that the values of D and E found are good estimates. Indeed, variations in these values of ca. 10% generate substantially different spectra that cannot be reconciled with the observed data. The simulation results for **3** and **4** were identical (Figure 5).

Despite the large number of Mn(II)−nitroxide radical complexes in the literature, there are very few powder EPR measurements corresponding to an isolated $S = 2$ state (resulting from coupled $S = {}^5/_2$ and $S = {}^1/_2$ units). The majority of systems either are extended structures incorporating local $S = 2$ states[10,16,42] or have two (or more) radicals bound to the Mn(II), leading to different spin states.[11,13,33,39−41] In a few cases, EPR spectra were discussed but not simulated;[43] the powder spectra for the related pyridine−nitronyl nitroxide complexes have not been reported in detail.[12,32] A comparison could technically be made with antiferromagnetically coupled Cu(II)−Mn(II) systems, for which detailed EPR measurements have been made and simulated, but these spectra are relatively different because of the varied geometries and magnetic centers involved.[44−46,47]

Conclusions

Paramagnetic phosphine oxide ligands have been introduced into the field of molecular magnetism. The reaction of *o*PONit with $Mn(hfac)_2$ gave a cis-chelated mononuclear system; changing the regiochemistry to *p*PONit generated binuclear molecular rectangles with $Mn(hfac)_2$. The powder EPR spectra of the complexes have been recorded and successfully simulated. The magnetic data showed strong Mn−radical coupling but weak ligand-mediated interactions, contrary to that observed for N-heterocycle ligands. The alteration of the ligand from a pyridine donor to a phosphine oxide and the subsequent change in magnetic pathway strength underlines the importance of ligand design in molecular magnetic materials. It is hoped that the use of triphenylphosphine oxide ligands (with their tetrahedral-cone topology) substituted with multiple radicals will increase the dimensionality of the superstructure formed on ligation with transition metals.

Acknowledgment. Financial support was provided by NSERC of Canada in the form of a postdoctoral fellowship (to D.B.L.) and by the TMR Research Network ERBFMRX-CT980181 of the European Union, entitled "Molecular Magnetism, from Materials toward Devices".

Supporting Information Available: For both structures complete tables of refined atomic coordinates, bond lengths and bond angles, hydrogen atom parameters, and anisotropic thermal parameters, in CIF format. This material is available free of charge via the Internet at http://pubs.acs.org.

IC990527G

(42) Caneschi, A.; Gatteschi, D.; Renard, J. P.; Rey, P.; Sessoli, R. *Inorg. Chem.* **1989**, *28*, 1976.
(43) Jiang, Z.-H.; Sun, B.-W.; Liao, D.-Z.; Wang, G.-L.; Donnadieu, B.; Tuchagues, J.-P. *Inorg. Chim. Acta* **1998**, *279*, 76.
(44) Mathoniere, C.; Kahn, O.; Daran, J.-C.; Hilbig, H.; Köhler, F. H. *Inorg. Chem.* **1993**, *32*, 4057.
(45) Banci, L.; Bencini, A.; Gatteschi, D. *Inorg. Chem.* **1981**, *20*, 2734.
(46) Paulson, J. A.; Krost, D. A.; McPherson, G. L.; Rogers, R. D.; Atwood, J. L. *Inorg. Chem.* **1980**, *19*, 2519.
(47) Bencini, A.; Gatteschi, D. *EPR of Exchange Coupled Systems*; Springer: Berlin, 1990.